

INFLUENCE OF CONFINEMENT ON THE TRANSITION VELOCITY OF SILICON CARBIDE

Olof Andersson, Patrik Lundberg and René Renström

FOI, Swedish Defence Research Agency, Defence & Security Systems and Technology Division Grindsjön,
SE-14725 Tumba, Sweden

In order to study the influence of a confining pressure on the transition velocity of ceramic targets, tests with unconfined and confined silicon carbide targets have been performed. The velocity interval within which transition occurred in the unconfined target was 1027 ± 23 m/s while confined targets had an interval of 1549 ± 19 m/s (previous test). This change in transition velocity corresponds to a difference in maximum contact pressure of 13 GPa (26 GPa at 1549 m/s versus 13 GPa at 1027 m/s). This means that a confining pressure of around 200 MPa enables a doubling of the loading of the ceramic target before penetration starts. The large influence of the confining pressure is explained via a simple fracture model showing that a small confining pressure drastically increases the surface load needed to extend macro cracks to critical dimensions.

INTRODUCTION

Interface defeat or dwell in ceramic targets was systematically studied and first reported by Hauver *et al.* [1,2] and later by Rapacki *et al.* [3]. Different matters concerning interface defeat have been dealt with in subsequent studies. For example, Lundberg *et al.* [4,5] determined the transition velocity (i.e., the maximum impact velocity at which interface defeat no longer can be sustained) for different target materials and La Salvia *et al.* [6] developed a micromechanical model to predict the influence of the ceramic microstructure on the performance of the ceramic material with respect to interface defeat.

In most of the experimental studies, the ceramic material was pre-stressed using a shrink fitted confinement. As the strength and fracture properties of ceramic materials show a pressure dependency, it should be expected that the transition velocity will depend upon the amount of confining pressure used. This effect has been studied using numerical simulations by Holmquist and Johnson [7]. Their simulations showed an increase in transition velocity with increasing confining pressure. Lately, experiments by

Holmquist *et al* [8] has shown that it is possible to achieve high transition velocities in silicon carbide (above 1600 m/s) without any use of confinement. This result indicates that the relation between confining pressure and transition velocity is not fully understood. In order to study the influence of confining pressure on the transition velocity, tests with unconfined silicon carbide cylinders have been performed. The experiments are similar to the ones performed in [5] except for the lack of confinement of the ceramic target. The results are interpreted using a simple model for a conical crack system which is initiated at the target surface close to the impact zone and propagates through the target during the interaction.

EXPERIMENTS

The experiments were performed using the reverse impact technique. Unconfined silicon carbide cylinders (SiC-B) with diameter 20 mm and length 20 mm were launched against stationary projectiles suspended in blocks of Divinycell (density 45 kg/m³). The projectiles were cylinders with length 120 mm and diameter 2 mm made of sintered tungsten alloy (Y925 from Kennametal Hertel AG). Figure 1 shows the projectile in its fixture in front of the muzzle of the gun. The target consisted of the ceramic cylinder, a supporting steel backing and a circular copper cover. The copper cover with diameter 20 mm and thickness 0.5 mm expanded in its central part to a cylinder with diameter 5.71 mm and thickness 8 mm. It was glued onto the ceramic cylinder along the rim. The geometry of the target is shown in Figure 2. The ceramic material was produced by Cercom Inc., USA, using pressure-assisted densification technique (PAD). The final cylinders were cut and ground from a larger plate.

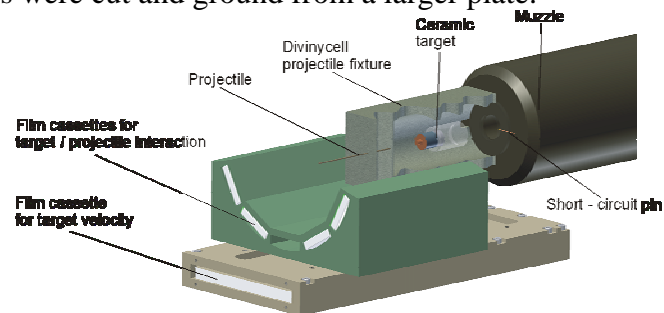


Figure 1. Experimental set-up.

The impact velocity and the penetration depth were evaluated from flash X-ray pictures. Trigger signals from a short-circuit pin mounted on the muzzle of the gun were used to trigger the flashes. To determine the impact velocity v_0 , two 150 kV X-ray flashes were used to depict the target before interaction with the projectile.

Four 450 kV X-ray flashes, positioned at the same distance from the barrel and radially separated by 30° were used to record the penetration process. The penetration depth P in the ceramic was determined from the X-ray pictures by use of image-processing techniques. From the flash X-ray data, the average penetration velocity u was obtained using linear least square fits.

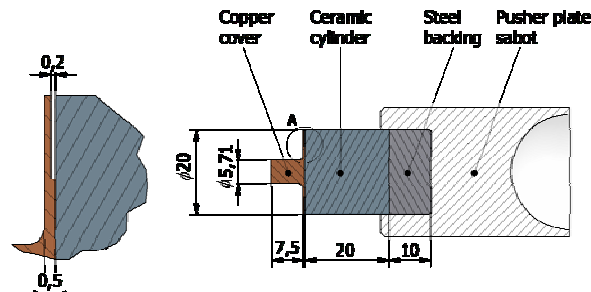


Figure 2. Ceramic target.

CONE CRACK MODEL

The driving force that geometrically directs a cone crack-extension is a complicated time-dependent stress field that develops around the surfaces of the crack. Here, as a first approximation, it is assumed that the crack will follow a trajectory of principal stresses so that one of these (in tension) is directed normal to the crack surface and the other two principal stresses directed along the surface according to the symmetric cylinder geometry. The radial extension of the crack is thereby assumed to be determined from the crack-intensity factor K_{Ic} of the ceramic material relative to the elastic stress field at the tip of the crack, as if the stress field was not divided by the crack.

Surface load and stress field in the ceramic

The model for the surface pressure load is taken from a measured pressure profile of a jet of water at low velocity on a flat surface [4]. The stress field $\sigma_{ij}(r, z)$ in the ceramic half-space of dimensionless co-ordinates r and z , resulting from the projectile under stationary interface defeat conditions is determined by the method of influence-function from a point-load by Boussinesq as

$$\sigma_{ij}(r, z) = \iint_{A(\varphi\rho)} \rho \sigma_{ij}(r, z, \varphi, \rho) d\varphi d\rho \quad (1)$$

where i, j , signifies r and z , A is the rotational-symmetric contact area of surface pressure, $\rho = r/a$ is the non-dimensional radius and $\sigma_{ij}(r, z, \varphi, \rho)$, defined negative in compression, is the stress field influence-function for a point load of intensity $p(\varphi, \rho)$

at a surface point (φ, ρ) . The stress field is thus dimensionless with respect to the maximum pressure p_0 of the pressure profile.

Approximate crack path and principal stress

For a high enough surface load, the crack will start at the surface of the ceramic target at the radius of maximum tensile radial stress. The crack starts as an axially symmetric cylinder (ring crack) since the radial stress at $z=0$ is a principal stress (friction-free surface). It is assumed that the ring crack will grow axially to a position below the surface where the direction of the principal tensile stresses changes. The crack will then gradually transform to a cone shaped crack surface with its normal directed as the tensile principal stress at this surface. The crack path is thus assumed to follow a direction, which is perpendicular to the local tensile principal stress as if this is not affected by the running crack. Although this is known to be a crude assumption of the process of an extending crack, it will serve as a model of the crack system studied. The crack path will then follow from the equation of direction as

$$\frac{dz_c}{dr} = \tan(\theta), \quad r > 0, z \geq 0 \quad (2)$$

where θ is the angle between the cone surface and the surface $z=0$, of the ceramic half-space and where

$$\tan(2\theta) = \frac{2\sigma_{rz}(r, z)}{\sigma_{rr}(r, z) - \sigma_{zz}(r, z)} \quad (3)$$

is determined from Equation (1). The principal tensile stress along the cone surface and directed normal to this can be determine from the equation

$$\begin{aligned} \sigma_1(r) = & \sigma_{rr}(r, z_c(r))\sin^2(\theta) - 2\sigma_{rz}(r, z_c(r))\sin(\theta)\cos(\theta) \\ & + \sigma_{zz}(r, z_c(r))\cos^2(\theta) \end{aligned} \quad (4)$$

Crack length and scaling

The stress concentration at the tip of an infinitely thin crack is defined as

$$K = \sigma\sqrt{\pi c} \quad (5)$$

where K , σ and c , are the dimensional stress intensity factor, a nominal stress (affecting the crack in its vicinity) and the length of the crack, respectively. The maximum stress intensity factor K_c of equation (5), index c indicating “critical”, is seen as a material property determining the maximum attainable stationary length c of a thin crack

in a given field (of nominal) stress surrounding the tip of the crack. With equation (5), rewritten in the form

$$\bar{\sigma}(r) = \frac{\bar{K}_c}{\sqrt{\pi a}} \frac{1}{\sqrt{\bar{c}(r)}} \quad (6)$$

where $\bar{K}_c = K_c / p_0$ is a constant with the dimension of $\text{length}^{1/2}$ and $\bar{\sigma} = \sigma / p_0$ and $\bar{c} = c / a$, are dimensionless variables, and with Eqs.(1-4), there is a system of equations to determine the possible stationary length of a cone-crack corresponding to a given load on the surface of the ceramic. The parameters of the system are K_c and ν , the critical stress intensity factor and the Poisson's ratio of the ceramic material, respectively, the projectile radius a and the distribution of load intensity, also involving projectile material density, strength and impact velocity. The system of equations (1-6) is solved numerically for the dimensionless length \bar{c} of crack surface by first solving equations (2, 3) numerically to get the expression (4) for $\bar{\sigma}_1$ and then determining the length \bar{c} of the crack by equation (6) with $\bar{\sigma}$ substituted by $\bar{\sigma}_1$.

Equations (1) to (4) are invariant with respect to geometrical dimensions, i.e., elastic conditions are expected to be the same, irrespective the length scale involved. Equation (6) (i.e. Equation (5)) is however not independent of length scale, instead the radius a of the projectile is a crucial dimensional parameter in this equation even in the case of an unlimited ceramic half-space. It is seen therefore, that equation (6) can be interpreted such that the effective critical stress intensity factor is decreasing by a factor $1/\sqrt{a}$ with increasing projectile radius, i.e., this factor of *crack resistance* of the ceramic material decreases with increasing scale in contrast to the otherwise scale-invariant elastic stress field. This means that the extension of a cone crack will be proportionally larger for a larger projectile as compared to linear scaling.

Influence of confinement on a finite ceramic target

The confinement (pre-stress) is expected to result in a higher penetration resistance of the target material. The influence of confinement is here studied by applying a radial pressure on the otherwise free cylindrical surface of a finite and thick ceramic target. A positive pressure q applied on the cylindrical surface of a long cylinder under elastic conditions, results in a constant radial stress equal to $-q$, i.e., a radial compressive stress in the cylinder. This will, firstly, decrease the maximum radial tensile stress in the ceramic surface by the amount of $-q$, which will admit a small increase of the surface load before a first surface ring-crack appears. Secondly, for a running crack, Equations (3) and (4) change to

$$\tan(2\theta) = \frac{2\sigma_{rz}(r, z)}{\sigma_{rr}(r, z) - q - \sigma_{zz}(r, z)} \quad (3.1)$$

and

$$\begin{aligned} \sigma_1(r) = & (\sigma_{rr}(r, z_c(r)) - q) \sin^2(\theta) - 2\sigma_{rz}(r, z_c(r)) \sin(\theta) \cos(\theta) \\ & + \sigma_{zz}(r, z_c(r)) \cos^2(\theta) \end{aligned} \quad (4.1)$$

when the radial stress $-q$ is superimposed. This added, radial compressive stress, $-q$, decreases the driving stress σ_1 of the crack and thus decreases the stationary length of a cone crack relative to the corresponding crack length for the unconfined case.

RESULTS AND DISCUSSION

Examples of X-ray pictures from impact tests above and below the transition velocity are shown in Figures 3-5. Figure 3 shows the development of interface defeat at an impact velocity below the transition velocity. The experiment shows that after radial flow had been established, it continues steadily for a long time.

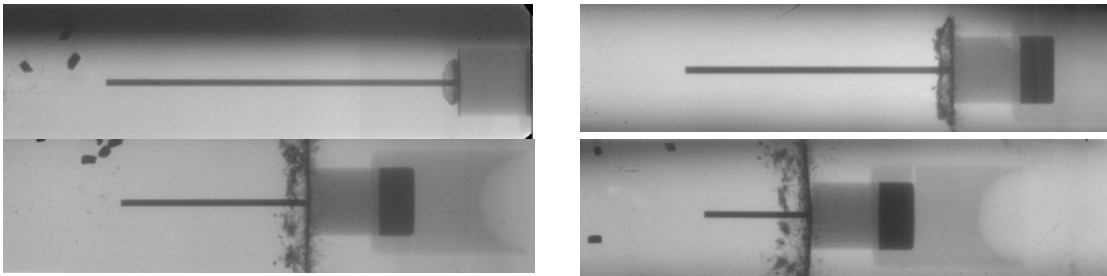


Figure 3. $v_0 = 1004$ m/s (8, 37, 65, 94 μ s)

At an impact velocity above the transition velocity, penetration occurs as shown in Figures 4 and 5. Even in these cases, a period of dwell could be observed on the X-ray pictures. The dwell period was relatively long (tens of μ s) compared to earlier tests at higher impact velocities with confined targets (3-5 μ s) [5].

The penetration of the unconfined ceramic target seems to be controlled by a combination of micro- and macro fracturing. The macro fracturing starts with a ring/cone crack which is initiated on the front surface of the ceramic. As the penetration proceeds, several different cone- and radial fracture systems develop. In all of the tests where penetration occurred, the penetration process is highly intermittent. This is probably a major source to the large scatter in the penetration velocities seen in Figure 6(a).

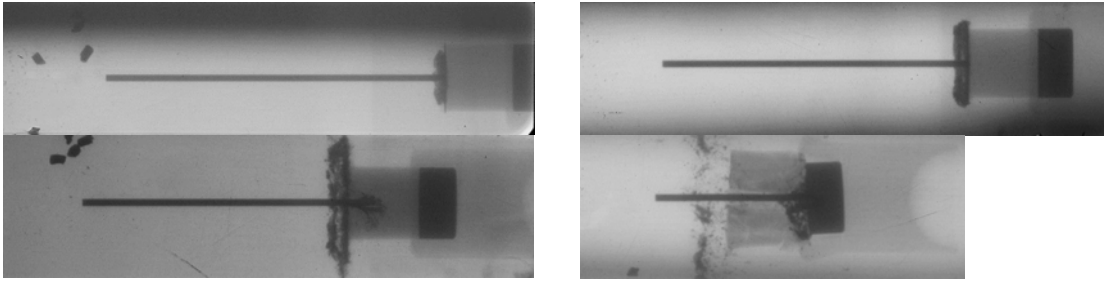


Figure 4. $v_0 = 1051$ m/s (14, 29, 43 and 100 μ s)

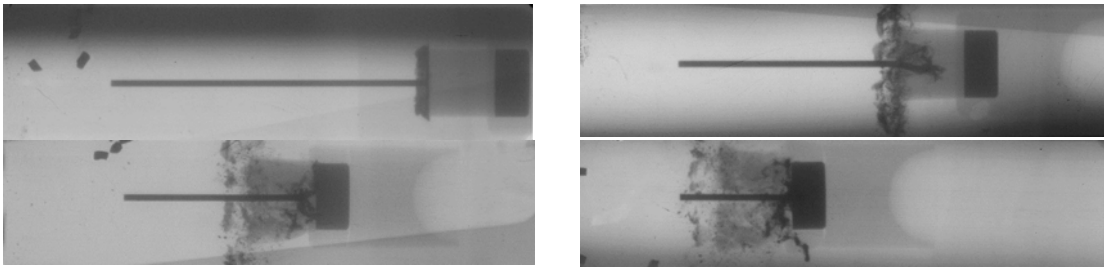


Figure 5. $v_0 = 1104$ m/s (21, 49, 78, 106 μ s)

The velocity interval within which transition occurred in the unconfined SiC-B target is 1027 ± 23 m/s. Previous tests with confined SiC-B targets [5] gave a transition velocity of 1549 ± 19 m/s, see Figure 6(a). This change in transition velocity corresponds to a maximum contact pressure drop of the order of 13 GPa (26 GPa at 1549 m/s versus 13 GPa at 1027 m/s). This means that a confining pressure of around 200 MPa [5] enables a doubling of the loading of the ceramic target before penetration starts. This can be explained by the simple model presented above. A small confining pressure drastically increases the surface load needed to extend a cone crack to a given length as shown in Figure 6(b). Assuming this mechanism is relevant for the break-down of the target, the diagram indicates how much confining pressure is needed to suppress the fracture mechanism. Using the experimental results for the unconfined case in Figure 6(a), the model estimates that a confining pressure of around 150 MPa is needed to reach a transition velocity of around 1600 m/s. This is in agreement with the results in [5].

The model also predicts that, apart from the confining pressure, scale also changes the surface load needed to extend a cone crack to given length. This is illustrated in Figure 6(c). Using the experimental results for the unconfined case in Figure 6(a), the model estimates that a reduction in scale by a factor of four is needed to reach a transition velocity of around 1600 m/s. These results are consistent with experimental data presented by Holmquist *et al* [8].

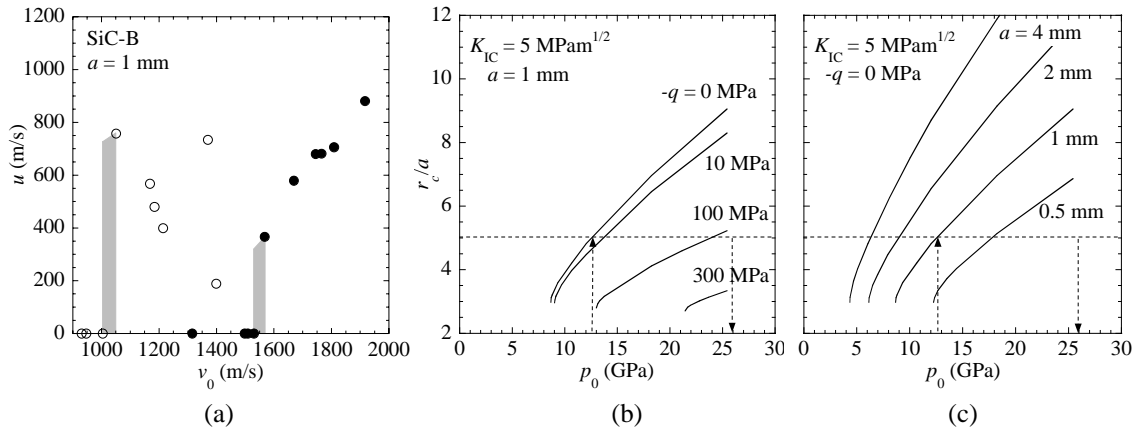


Figure 6. (a) Evaluated penetration velocities u versus impact velocity v_0 for the unconfined target (open symbols) and the confined target (filled symbols), respectively. Influence of pre-stress (b) and scale (c) on cone crack length (r -direction) versus maximum contact pressure.

It is reasonable to assume that all types of macro-fracturing will show the same principle behaviour as the ring crack system studied here. If macro-fracturing is an important mechanism for controlling the transition velocity of a ceramic target, the model above is a helpful tool to interpret the influence of scale and confining pressure.

REFERENCES

- [1] Hauver GE, Netherwood PH, Benck RF, Kecskes LJ. Ballistic performance of ceramic targets. Army Symposium on Solid Mechanics, USA, 1993
- [2] G. E. Hauver, P. H. Netherwood, R. F. Benck and L. J. Kecskes. Enhanced ballistic performance of ceramic targets. 19th Army Science Conference. USA 1994.
- [3] E. J. Rapacki, G. E. Hauver, P. H. Netherwood and R. F. Benck, Ceramics for armours- a material system perspective. 7th Annual TARDEC Ground Vehicle Survivability Symposium. USA 1996.
- [4] Lundberg P, Renström R, Lundberg B. Impact of metallic projectiles on ceramic targets: transition between interface defeat and penetration. Int J Impact Engng 2000;24:259-275.
- [5] P. Lundberg, B. Lundberg, Transition between interface defeat and penetration for tungsten projectiles and four silicon carbide materials. Int J Impact Engng 2005;31:781-792.
- [6] J. C. LaSalvia, E. J. Horwath, E. J. Rapacki, C. J. Shih and M. A. Meyers. Microstructural and micromechanical aspects of ceramic/long-rod projectiles inter-actions: dwell/penetration transitions. In Fundamental Issues and applications of Shock-Wave and High-Strain-Rate Phenomena, 437-446, edited by K. P. Staudhammer, L. E. Murr and M. A. Meyers, Elsevier Science, New York, (2001).
- [7] T. J. Holmquist and G. R. Johnson. Modelling projectile impact onto pre-stressed ceramic targets. J. Phys. IV, France, 110, 597-602 (2003).
- [8] T. J. Holmquist, C. E. Anderson Jr and T. Behner. Design, analysis and testing of an unconfined ceramic target to induce dwell. 22nd International Symposium on Ballistics, Vancouver, BC, Canada, 14-18 November 2005.